ELSEVIER

Materials Science and Engineering A261 (1999) 165–168

MATERIALS SCIENCE & ENGINEERING A

Atomistic potentials for the molybdenum–silicon system

M.I. Baskes

Materials and Engineering Sciences Center, Materials Reliability Department Sandia National Laboratories, Livermore, CA 94551-0969, USA

Abstract

Using a modified version of the Embedded Atom Method (EAM) that includes angular forces, potentials are developed for the Mo/Si system. Previously developed potentials for Mo and Si are used. The cross potential is fit to properties of $MoSi_2$, Mo_3Si and Mo_5Si_3. Predictions are presented for phase stability, lattice constants, elastic constants and point and planar defect energies. In general the agreement with experiment is good, but the predicted lattice constants are somewhat greater than experiment.

Keywords: Atomistic potentials; Molybdenum–silicon system; Lattice constants

1. Introduction

To date atomistic potentials for the Mo/Si system have not been developed. Two significant reasons have limited their development: the complicated bonding found in these intermetallics and the complex crystal structures formed. First principles calculations [1,2] have been performed, but these calculations are unable to handle the large number of atoms necessary to evaluate the interfaces or defects that determine the mechanical properties of engineering materials.

Recently we have shown that a modification of the well-known Embedded Atom Method (EAM) can be made to broaden its applicability to many types of bonding by including angular forces through the background electron density [3,4]. Specifically using this method, the thermodynamics of both solid and liquid phases of tin have been predicted quantitatively [5]. These phases include both metallic and covalent bonding.

Continuing along this path, modified EAM (MEAM) potentials for the Mo/Si system have been developed. Using previously developed MEAM potentials for Mo and Si [3,6], the four parameters needed to perform calculations of Mo–Si intermetallics have been determined. Experimental data on three intermetallic compounds, $MoSi_2$, Mo_3Si and Mo_5Si_3 has been incorporated in the development of the potentials. The validity of the potentials has been evaluated by calculating the energetic, structural and elastic properties of the above compounds as well as many other metastable Mo–Si phases. In addition, the energetics and structure of point defects and planar defects, i.e. surfaces and faults, have been calculated. In all cases detailed comparison with experiment has been made when possible.

2. Theory

The EAM formulation is well known [7,8] and will not be repeated here. Similarly the MEAM has also been fully documented in the literature [3,9]. A minor modification to the form of the partial electron densities is instituted in this work and is discussed in the Appendix A. The parameters used are given in Table 1. Parameters for Mo and Si are taken from the literature [3,6] with the exception of $t^{(1)}$ which is modified as discussed in the Appendix A. The reference structure for the Mo/Si system is taken as the B1 or NaCl structure. There are four parameters to be determined, E_c, r_e and α for the B1 structure and ρ_0^a for Mo. These parameters are fit to the experimental heats of forma-

0921-5093/99/$ - see front matter
PII: S0921-5093(98)01062-4

Table 1
Parameters for the MEAM potentials[a]

	E_c	r_e	α	A	$\beta^{(0)}$	$\beta^{(1)}$	$\beta^{(2)}$	$\beta^{(3)}$	$t^{(1)}$	$t^{(2)}$	$t^{(3)}$	ρ_0^a
Mo	6.81	2.73	5.85	0.99	4.48	5.0	1.0	1.0	5.00	9.34	−2.9	1.60
Si	4.63	2.35	4.87	1.00	4.40	5.5	5.5	5.5	2.05	4.47	−1.8	2.05
MoSi	5.92	2.70	5.80	—	—	—	—	—	—	—	—	—

[a] Values listed are the cohesive energy E_c (eV), the equilibrium nearest neighbor distance r_e (Å), the exponential decay factor for the universal energy function α, the scaling factor for the embedding energy A, the exponential decay factors for the atomic densities $\beta^{(1)}$, the weighting factors for the atomic densities $t^{(1)}$ and the density scaling factor ρ_o^a.

Table 2
Angular screening parameters for the MEAM potentials

	Mo–Mo–Mo	Mo–Si–Mo	Si–Mo–Mo	Si–Si–Mo	Si–Mo–Si	Si–Si–Si
C_{max}	2.6	2.6	2.8	2.8	2.8	2.8
C_{min}	2.0	2.0	2.0	2.0	0.8	0.8

tion and lattice constants of the three stable Mo/Si compounds and the bulk modulus of $MoSi_2$. Angular screening as implemented in Baskes et al. [9] was used to limit the range of the functions. The parameters used are given in Table 2. In addition a radial cutoff of 4.3 Å was used to facilitate computation. The value chosen for the radial cutoff was found to be unimportant.

The MEAM functions are shown in Figs. 1–3. Note the simplicity of the functions. The rapid decrease in the partial electron density (Fig. 3) for Mo is due the cutoff of the functions at 4.3 Å.

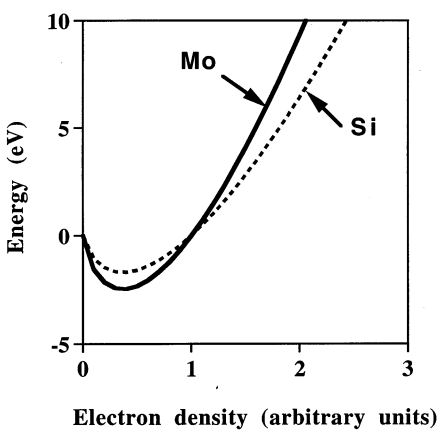

Fig. 1. Embedding energy as a function of background electron density.

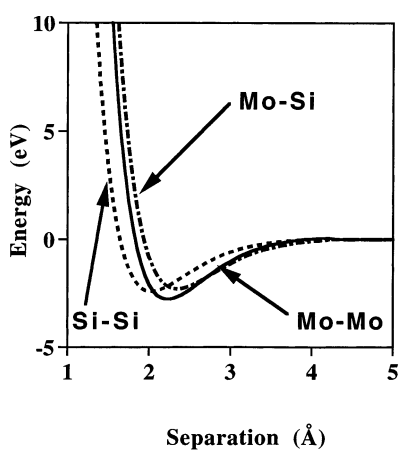

Fig. 2. Pair potential energy as a function of atomic separation.

3. Results

The calculated phase stability and structural properties of the three stable phases are presented in Table 3. The calculated heat of formation, ΔE, agrees reasonably well with experiment (Fig. 4). On the other hand, the calculated lattice constants are uniformly greater than experiment by as much as 12%. It is most likely that the failure to be able to fit both the lattice parameter and the structural energies simultaneously reflects a deficiency in MEAM to handle the transition from metallic to covalent bonding. In spite of our inability to

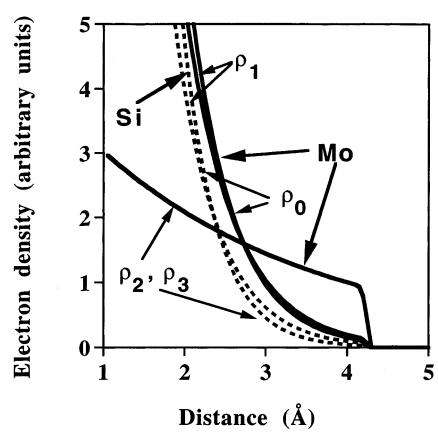

Fig. 3. Partial electron densities as a function of distance.

Table 3
Calculated values of the energetics and structural parameters of the three stable intermetallic phases of the Mo/Si system[a]

	$MoSi_2$	Mo_3Si	Mo_5Si_3
Crystal structure	C11b	A15	$D8_m$
ΔE (eV atom^{-1})	0.41* (0.44[b])	0.18* (0.29[b])	0.40* (0.39[b])
a (Å)	3.59* (3.20[c])	5.20* (4.89[c])	10.64* (9.64[c])
c (Å)	8.42* (7.86[c])	—	5.08* (4.91[c])
c/a	2.35* (2.46[c])	—	0.48* (0.51[c])
Internal coordinates	0.33* (0.33[c])		0.06* (0.075[c])
			0.25* (0.224[c])
			0.20* (0.165[c])

[a] Experimental values are shown in parentheses. Values denoted with an asterisk have been fit to experiment. All other values are predictions of the model.
[b] Reference [10].
[c] Reference [11].

Table 4
Calculated values of the elastic constants of the three stable intermetallic phases of the Mo/Si system[a]

	$MoSi_2$	Mo_3Si	Mo_5Si_3
B (GPa)	210* (210[b])	256	213 (243[c])
C_{11} (GPa)	252 (417[b])	641	326 (446[c])
C_{33} (GPa)	510 (515[b])	—	448 (390[c])
C_{12} (GPa)	145 (104[b])	63	141 (174[c])
C_{13} (GPa)	148 (84[b])	—	134 (140[c])
C_{44} (GPa)	26 (204[b])	404	110 (110[c])
C_{66} (GPa)	133 (194[b])	—	153 (140[c])
G (GPa)	75 (191[b])	358	121 (94[c])
E (GPa)	202 (440[b])	732	305 (249[c])
v	0.34 (0.15[b])	0.02	0.26 (0.33[c])

[a] Experimental values are shown in parentheses. Values denoted with an asterisk have been fit to experiment. All other values are predictions of the model. Isotropic values are Voigt averages of the single crystal data.
[b] Reference [12].
[c] Reference [13].

predict more accurate lattice constants, the c/a ratio agrees quite well with experiment. The internal coordinates are also in excellent agreement with experiment. In order to investigate the robustness of the model a number of calculations of the phase stability of other Mo/Si phases was performed. Phases considered were A_{15}, C11b, $D8_m$, B1, B2, C40, $B8_8$, L_{10} and L_{12}. The results of these calculations are shown in Fig. 4. Here we see agreement with the experimental phase diagram is perfect with two exceptions. The $MoSi_3$ (L_{12}) is predicted to be stable in disagreement with experiment while Mo_3Si (A15) is predicted to be unstable with respect to decomposition to Mo_5Si_3 and Mo. Small changes in lattice stability (~ 10 meV) would correct these discrepancies.

The elastic constants of the experimentally stable phases are given in Table 4. Also shown in the table are the Voigt average elastic constants. The predicted elastic constants for $MoSi_2$ agree fairly well with experiment. However there is a significant under prediction of C_{11} and C_{44} which lead to rather poor agreement of the isotropic elastic constants with experiment. On the other hand the predictions for Mo_5Si_3 agree remarkably well with experiment. The single crystal elastic constants for Mo_3Si lead to a rather low value of the Poisson ratio.

The predictions for a number of simple planar defects are presented in Table 5. Calculated surface energies in the range of 1–3 J m^{-2} appear to be reasonable for these high temperature materials. The two entries for $MoSi_2$ represent different surface terminations which lead to a similar surface energy. The calculated fault energies are reasonably close to the experimental values which have a large uncertainty.

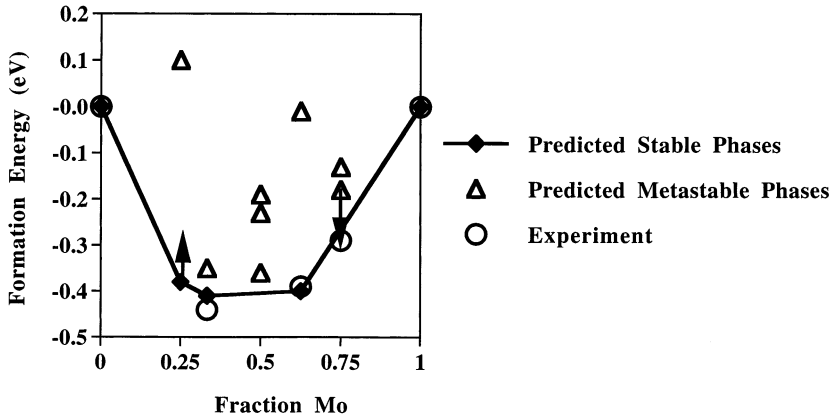

Fig. 4. Formation energy relative to elemental Mo and Si of various compounds as a function of stoichiometry.

Table 5
Calculated energies of planar defects in the three stable intermetallic phases of the Mo/Si system[a]

	$MoSi_2$	Mo_3Si	Mo_5Si_3
(100) surface (mJ m^{-2})	1790	2850	2110
(001) surface (mJ m^{-2})	2015, 2100	—	2510
1/4<111]{110}SISF (mJ m^{-2})	209 (261[b], 365[c])	—	—
1/6<331]{013}APB (mJ m^{-2})	1313 (824[d])	—	—

[a] Experimental values are shown in parentheses.
[b] Reference [14].
[c] Reference [15].
[d] Reference [16].

Table 6
Calculated energies of point defects in the three stable intermetallic phases of the Mo/Si system[a]

	$MoSi_2$	Mo_3Si	Mo_5Si_3
Mo vacancy (eV)	12.0	9.4	9.7, 6.6
Si vacancy (eV)	5.8	7.1	8.0, 7.4
Si on Mo site (eV)	6.3	3.1	3.6, 0.9
Mo on Si site (eV)	−1.2	1.6	0.0, −0.3
Anti-site defect (eV)	5.1	4.7	0.6 to 3.6

[a] Values except for the anti-site defect are relative to isolated atoms at infinity.

Point defect calculations are presented in Table 6. The energies of the point defects are presented relative to isolated atoms at infinity. For example, the energy listed for a Mo vacancy in an intermetallic is the difference in energy between an alloy with one Mo atom removed and the perfect alloy. To compare with experimental data (which is not currently available) this number must be adjusted by the chemical potential of Mo. The multiple entries for Mo_5Si_3 occur because there are two types of sites for both Mo and Si in this alloy. Also presented are the energies calculated for replacing a Mo atom by a Si atom and vice versa. Again these energies are relative to isolated atoms at infinity. They must be corrected by the appropriate chemical potentials. Note that the calculations predict the possibility of a low energy (0.6 eV) anti-site defect. The point defect energetics will be useful in determining the disordering of these systems at high temperature.

Acknowledgements

This work was supported by the US Department of Energy, Office of Basic Energy Sciences, Division of Materials Sciences under the Center for Synthesis and Processing.

Appendix A

Previous MEAM calculations have used partial electron densities that were not orthogonal. The present work used partial electron densities that were Legendre polynomials. The only difference is that a second term is added to $\rho^{(3)}$. The new equation is:

$$(\rho^{(3)})^2 = \sum_{\alpha,\beta,\gamma}\left[\sum_i \rho^{a(3)}(r^i)\frac{r^i_\alpha r^i_\beta r^i_\gamma}{(r^i)^3}\right]^2 - \frac{3}{5}\sum_\alpha\left[\sum_i \rho^{a(3)}(r^i)\frac{r^i_\alpha}{r^i}\right]^2 \quad \text{(A1)}$$

See Baskes et al. [9] for a description of the nomenclature. To use previous MEAM functions with the new formulation the value of $t^{(1)}$ must be replaced by $t^{(1)} + 3/5t^{(3)}$.

References

[1] M. Alouani, R.C. Albers, M. Methfessel, Calculated elastic constants and structural properties of Mo and $MoSi_2$, Phys. Rev. B 43 (1991) 6500–6509.
[2] A.K. McMahan, J.E. Klepeis, M.V. Schlifgaarde, M. Mesthfessel, Bonding in the molybdenum silicides, Phys. Rev. B 50 (1994) 10742—10760.
[3] M.I. Baskes, Modified embedded—atom potentials for cubic materials and impurities, Phys. Rev. B 46 (1992) 2727–2742.
[4] M.I. Baskes, R.A. Johnson, Modified embedded atom potentials for hcp metals, Model. Simul. Mater. Sci. Eng. 2 (1994) 147–163.
[5] R. Ravelo, M. Baskes, Equilibrium and thermodynamic properties of grey, white and liquid tin, Phys. Rev. Lett. 79 (1997) 2482–2485.
[6] M.I. Baskes, Calculation of the behavior of Si–Ad-dimers on Si (001), Model. Simul. Mater. Sci. Eng. 5 (1997) 149–158.
[7] M.S. Daw, M.I. Baskes, Embedded—atom method: derivation and application to impurities, surfaces and other defects in metals, Phys. Rev. B 29 (1984) 6443.
[8] M.S. Daw, S.M. Foiles, M.I. Baskes, The embedded atom method: a review of theory and applications, Mater. Sci. Rep. 9 (1993) 251–310.
[9] M.I. Baskes, J.E. Angelo, C.L. Bisson, Atomistic calculations of composite interfaces bisson, Model. Simul. Mater. Sci. Eng. 2 (1994) 505–518.
[10] E.A. Brandes, Smithells Metals Reference Book, 6, Butterworths, London, 1983.
[11] P. Villars, L.D. Calvert, Pearson's Handbook of Crystallographic Data for Intermetallic Phases, vol. 4, ASM International, Materials Park, OH, 1991.
[12] M. Nakamura, S. Matsumoto, T. Hirano, Elastic constants of $MoSi_2$ and WSi_2 single crystals, J. Mater. Sci. 25 (1990) 3309–3313.
[13] F. Chu, D.J. Thoma, K. McClellan, P. Peralta, Mo_5Si_3 Single Crystals: Physical Properties and Mechanical Behavior, in: J.J. Petrovic, M.A. Hyannis (Eds.), High Temperature Structural Silicides, 1998.
[14] D.J. Evans, S.A. Court, P.M. Hazzledine, H.L. Fraser, Dislocation dissociation in the intermetallic Compound $MoSi_2$, Phil. Mag. Lett. 67 (1993) 331.
[15] K. Ito, H. Inui, Y. Shirai, M. Yamaguchi, Plastic deformation of $MoSi_2$ single crystals, Phil. Mag. A 72 (1995) 1075–1097.
[16] K. Ito, T. Yano, T. Nakamoto, H. Inui, M. Yamaguchi, Plastic deformation of $MoSi_2$ and WSi_2 single crystals and directionally solidified $MoSi_2$-based alloys, Intermetallics 4 (1996) 119–131.